TWO-NEUTRON STRIPPING REACTIONS LEADING TO THE ^{153}Sm, ^{178}Yb and ^{180}Hf NUCLEI

TWO-NEUTRON STRIPPING REACTIONS LEADING TO THE ^{153}Sm, ^{178}Yb AND ^{180}Hf NUCLEI

by

IGOR GEORGE NOWIKOW

A Thesis

Submitted to the Faculty of Graduate Studies

in Partial Fulfilment of the Requirements

for the Degree

Master of Science

McMaster University

March 1979

MASTER OF SCIENCE — McMASTER UNIVERSITY

(PHYSICS) — Hamilton, Ontario

TITLE: Two-Neutron Stripping Reactions Leading to the ^{153}Sm, ^{178}Yb and ^{180}Hf Nuclei.

AUTHOR: IGOR GEORGE NOWIKOW, B.Sc. (McMaster University)

SUPERVISOR: DR. D.G. BURKE

NUMBER OF PAGES: vi, 50

Abstract

The (t,p) reaction has been performed on targets of ^{151}Sm, ^{176}Yb and ^{178}Hf. The experiment was performed with 15 MeV tritons. The outgoing protons were analyzed with the Enge split-pole spectrograph. Angular distributions were measured for all three nuclei with special emphasis being placed on L=0 transitions.

The angular distributions for the $^{151}Sm(t,p)^{153}Sm$ reaction showed that the distribution of L=0 strength among the low-lying states is not consistent with expectations based on the detailed wavefunctions for ^{151}Sm and ^{153}Sm calculated by two independent groups; Katajanheimo and Hammaren (1978) and Rekstad *et al.* (1978). The distributions also showed that the total L=0 strength, summed over the four observed states in ^{153}Sm, is much less than for neighbouring nuclei.

Angular distributions of the (t,p) reaction on ^{176}Yb and ^{178}Hf targets showed strong L=0 transitions to levels at $\sim$ 1.3 MeV excitation. It is believed that the N=108 energy gap in the Nilsson diagram is the cause of the large L=0 strength observed. At present no quanitative calculation has reproduced the observed phenomenon, however a calculation based on the Volkov model is presently being considered.

ACKNOWLEDGEMENTS

I would like to thank Dennis Burke, my supervisor for his patience, his guidance, his great sense of "blond" humor, and most important of all, his friendship.

Special thanks should also go to Esko "Camaro" Hammaren, "Alberta" Lee and the "Mighty" Arif Khan, who have helped me throughout various stages of my graduate career .

Edna Williams deserves a hardy applause and a very deep bow for her masterful job of typing (and retyping) this thesis.

I would also like to thank Helen Yardley for her many hours of pain-staking work in counting the photographic plates. As well, thanks should go to Suzanna den Bleker for those many last minute corrections in the thesis that seemed to amount to hours.

And finally (but certainly not the least) a sincere thanks to everyone in the lab; the profs, the post-docs, the grads, the students,"block n' tackle Williams", "five-putt" Starkie,"Triton"Peng,"Jaguar" John and the rest of the merry band of henchmen and rogues for making this period of life a pleasant and most memorable one!!

Finanacial support was provided by the National Research Council of Canada.

TABLE OF CONTENTS

LIST OF FIGURES

LIST OF TABLES

CHAPTER I

INTRODUCTION

The isotopes of Sm are of particular interest to nuclear physicists due to the somewhat abrupt change of nuclear deformation from neutron number N=88 to N=90. The existence of typical vibrational structure in ^{150}Sm (N=88) characteristic of spherical even-even nuclei, and rotational bands in ^{152}Sm (N=90) typical of deformed even-even nuclei bear out this fact (Bjerregaard et al. 1966). The odd-even nucleus ^{151}Sm (N=89) is of interest because of its location between the two different deformations of its neighbours.

The ^{153}Sm nucleus, which is under consideration in this thesis, is the residual nucleus in the (t,p) reaction on ^{151}Sm. It has been studied via decay processes and single-nucleon transfer reactions (Kenefick et al. 1965, Bennett et al. 1971). However, there have remained ambiguities in the wavefunctions of single neutron states which could be clarified using the (t,p) reaction. As well, some insight about the ground state wavefunction of the ^{151}Sm target nucleus can be expected.

To understand why the reaction is useful in probing the neutron states under consideration a brief summary of the properties of the reaction are in order. In two-neutron transfer reactions performed on even-even rare earth nuclei it was found that ground state to ground state transitions dominated as long as both nuclei were of similar deformation. However appreciable hindrance was observed for the L=0 strength in reactions connecting ground states of isotopes with 88 and 90 neutrons. Instead a large amount of the L=0 strength went to an excited state presumed to have comparable deformation to that of the

ground state of the target nucleus (Bjerregaard et al. 1966) (McLatchie et al. 1970).

For the odd mass deformed nuclei the L=0 strength is observed to go primarily to the same Nilsson orbital as the target ground state (Burke et al. 1975). In cases where Coriolis coupling or other mixing effects are significant, the L=0 strength is found to be spread over levels containing admixtures of the ground-state configuration of the target (Burke et al. 1975). Thus the (t,p) reaction allows one to test the wavefunctions of the ground state of the target nucleus, or the wavefunctions of the residual nucleus assuming that the nature of the ground state is known. Since the ground state of ^{151}Sm has been determined to be $5/2^-$ (Robertson et al 1971, Nelson et al. 1973), previously reported and possibly new $5/2^-$ states in ^{153}Sm will be under consideration in this study.

Theoretical calculations have been performed on both nuclei by two independent research groups, Rekstad et al. (1978) and Katajanheimo and Hammaren (1978). Both these studies involve Nilsson calculations using a particle-rotor model. However the choice of potential functions as well as choices of independent parameters differed between the studies. Although both groups agree on the general structures of the ^{151}Sm and ^{153}Sm nuclei, the Coriolis coupling amplitudes differed appreciably. The results of this experiment may allow one to test the wavefunctions of the $5/2^-$ states predicted by these calculations.

This study also presents the results of (t,p) reactions leading to the even-even nuclei ^{178}Yb and ^{180}Hf. In this part of the rare earth region one finds an energy gap between the $9/2^+[624]$ and $7/2^-[503]$ Nilsson orbitals corresponding to neutron numbers N=108 and N=110. It has been thought that this gap presents a situation similar to that of a closed shell, as in the case of

^{208}Pb (Broglia and Riedel 1967) in which the $^{+}0_{n}$ states contain large (t,p) strengths (Nathan 1968). It is believed that the ^{178}Yb and ^{180}Hf spectra will exhibit such features. Also as a result of this experiment information on levels in ^{178}Yb can now be presented for the first time. There are no nuclear structure data for excited states of ^{178}Yb in the Nuclear Data Sheets.

CHAPTER II

THEORETICAL BACKGROUND

Nuclear structure studies proper involve a vast and complex world of many body systems. To circumvent the massive computational difficulties involved in correlating hundreds of nucleons interacting with each other by some force or forces, certain models were formulated using simplifying assumptions which were hopefully not too restrictive. However no model as yet describes successfully all the experimentally observed results.

2.1 Shell Model

The basic assumption of this model is that the nucleons are independent particles in orbits determined by an averaged interaction potential of all the nucleons. To explain the observed magic numbers a spin-orbit term is added whereby the single $n\ell$ states of the nucleon are now split into a $j = \ell \pm 1/2$ doublet with the state of larger j having the lower energy.

The Extreme Single Particle model assumes that the neutrons and protons fill independent shells. The nucleon pairs couple to angular momentum J=0 up to the last nucleon, which then determines the nuclear properties of the nucleus.

2.2 Collective Motion

In the region of interest in this study the nuclei are found to have large quadrupole moments which cannot be explained by the shell model. Instead one must consider the co-ordinated motions of many nucleons and hence the postulation of collective models.

A basic concept in collective motion is that the correlation of nucleons

causes a slowly changing space pattern with respect to the single particle motion. Thus the potential does not change much during the single particle period and it now appears that the particle is moving in a deformed potential. It should be noted that this assumption is made more out of convenience than of general validity.

In the simplest model a nucleus is considered to be a charged liquid drop. The excitation modes arise from small oscillations about the equilibrium spherical shape. The Hamiltonian of the drop is;

$$H = T + V = \frac{1}{2}\sum_{\lambda\mu} B_\lambda |\dot{\alpha}_{\lambda\mu}|^2 + \frac{1}{2}\sum_{\lambda\mu} C_\lambda |\alpha_{\lambda\mu}|^2$$

where the collective motions have been expressed by letting $\alpha_{\lambda\mu}$ vary with time. The two terms in the Hamiltonian correspond to the kinetic and potential energies. After quantization of $\alpha_{\lambda\mu}$ the eigenvalues become;

$$E_N = \hbar\omega \sum_\mu (n_\mu + \frac{1}{2})$$

the familiar energy spacings of the harmonic oscillator.

When considering deformed rotating nuclei, the axes of the nucleus now change with time. In this case it is easier working with Euler angles of the principal axes of the nucleus with respect to the fixed axes. Then through a series of these angular transformations, simplifying definitions and some not too trivial algebra one obtains the rotational Hamiltonian

$$H = T_\beta + T_\gamma + \sum_{K=1}^{3} \frac{L_K^2}{2\mathcal{I}_K} + V(\beta,\gamma)$$

where β is the measure of the total nuclear deformation and γ is a measure of the asymmetry of the nucleus. Here $\mathcal{I}_K$ is the effective moment of inertia and L_K is the component of angular momentum along the K axis. The potential $V(\beta,\gamma)$ actually

determines the type of spectrum one can expect.

In the more general case, rotations and vibrations must be coupled as $\mathcal{I}_K$ is a function of both β and γ.

For the even-even nuclei possesing a well localized deformation in the β-γ plane the normalized rotational wavefunctions are given by

$$|JMK\rangle = \left[\frac{2J+1}{16\pi^2(1+\delta_{K,0})}\right]^{1/2} (D^J_{MK} + (-)^J D^J_{M,-K})$$

$$\text{and} \quad E = \langle JMK | \Sigma \frac{L_K}{2\mathcal{I}_K} | JMK\rangle$$

$$= \frac{\hbar^2 J(J+1) - K^2}{2\mathcal{I}} + \frac{\hbar^2 K^2}{2\mathcal{I}_3} .$$

For the case of $K^\pi = 0^+$, as occurs for example in the ground state rotational band, the energy spacings are given by,

$$E_J = \frac{\hbar^2}{2\mathcal{I}} \quad J(J+1)$$

where J takes on the values 0, 2, 4 ... . In general K need not equal zero. In such bands, J takes on all values greater than or equal to K. Taking into consideration the pairing force which is especially strong for the ground state one can write the energy approximately as,

$$E = \frac{\hbar^2}{2\mathcal{I}} \quad J(J+1) + \langle E_{PAIR}\rangle$$

where for the rare earth region $\langle E_{PAIR}\rangle \approx -2$ MeV. Thus one can see that the ground state of the even-even nucleus is lowered in energy by 2 MeV.

For the case of an odd-even nucleus one must consider the coupling of collective modes to single particle states. For these nuclei the rotational

levels are built on various single-particle excitations. The complete wave equation for such a system is taken to be;

$$(T_{ROT} + \sum_p H_p)\ \psi = E\ \psi$$

where

$$T_{ROT} = \sum_{K=1}^{3} \frac{(J_K - j_K)^2}{2\mathcal{I}_K} \quad .$$

In expanding T_{ROT} for the case of nuclei with axial symmetry; $\mathcal{I}_1 = \mathcal{I}_2 = \mathcal{I}$ and $\mathcal{I}_3 \neq \mathcal{I}$. If one designates j_3 as Ω, then the rotational kinetic energy becomes,

$$T_{ROT} = \frac{\hbar^2}{2\mathcal{I}} [J(J+1) + \vec{j}^2 - 2\vec{J}\cdot\vec{j} - (K-\Omega)^2] + \frac{\hbar^2}{2\mathcal{I}_3} (K-\Omega)^2 \quad .$$

This further simplifies, as $K=\Omega$ for the axial symmetric case. The $2\vec{J}.\vec{j}$ term is analogous to the classical case of the potential energy of the Coriolis force on a particle. To first order this term is found to mix states with $\Delta K=1$ in cases where the states of the same J and different K are close in energy.

2.3 Nilsson Model

To obtain an understanding of the single particle states outside the deformed core, Nilsson proposed that the nucleons move in a potential shaped like the nucleus (Nilsson, 1955). The deformed potential he chose is of an anisotropic harmonic oscillator with axial symmetry. The Nilsson Hamiltonian is,

$$H_N = \hbar\omega \{\frac{1}{2}(-\nabla^2 + \rho^2) + \frac{4}{3}\frac{\pi}{5}\delta\rho^2 Y_2^o - 2K\vec{\ell}\cdot\vec{s} - \mu K\vec{\ell}\cdot\vec{\ell}\}$$

where the ℓ^2 term is added to depress the high angular momentum states, the $\vec{\ell}.\vec{s}$ term performs its usual function of splitting the $j = \ell \pm \frac{1}{2}$ degeneracy, the Y_2^o term introduces a deformation into the potential,

$$\rho^2 = \frac{m\omega_o(\delta)\, r^2}{\hbar} \quad .$$

The simple harmonic

oscillator part of the potential is given by the $(-\nabla^2+\rho^2)$ term. For this system it is convenient to use the $|N\ell j\Omega>$ basis wavefunctions representing simple single particle shell model states. In the limit of large deformations, ℓ_z, N_z, σ_z become constants of motion (where z refers to the body axis system) and are represented by corresponding quantum numbers Λ, n_z and Σ. Thus the Nilsson orbitals are labelled by these numbers in the following manner; $\Omega^{\pi}[Nn_z\Lambda]$ where π is the parity and equal to $(-1)^N$.

2.4 Two-Nucleon Transfer Reactions

Two-nucleon transfer reactions and specifically the two-neutron stripping reaction is a highly selective process favouring those states having a large parentage based on the target in its ground state.

For single and two-nucleon transfer reactions the angular distributions are characterized by the orbital angular momentum transferred in the reaction. For the (t,p) reaction the orbital angular momentum is carried by two neutrons and as a consequence many different configurations of the two may contribute. Thus the form factor is a coherent sum over these shell model configurations. However, it is found that the triton wavefunction is space symmetric and therefore for the neutrons S=0 and L=J (Hintz, 1964). Thus the angular distributions give directly the J to which the pair has been coupled.

It is also found that the greatest reaction cross-section occurs for the transfer of the two neutrons in a relative S state coupled to L=0. The resulting high degree of pair correlation results in a form factor in which all the terms add in phase (Glendenning 1964). In general strong ground state to ground state transitions result, especially in even-even nuclei. However there are exceptions to this case, including the ^{178}Yb and ^{180}Hf isotones to which part of this study is dedicated.

CHAPTER III

EXPERIMENTAL DETAILS

3.1 Introduction

Using the newly installed McMaster tritium source, 15 MeV triton beams were obtained for the purpose of studying two-neutron transfer reactions on ^{151}Sm, ^{176}Yb and ^{178}Hf targets. An Enge split-pole magnetic spectrograph was used to analyze the reaction products at various angles. Photographic emulsions were used to record the tracks of the reaction protons. The tracks left in the emulsion were later scanned to locate peak positions and determine energies and cross-sections for levels populated in the residual nuclei.

For the purpose of determining absolute cross-sections a Si(Li) monitor detector, 1 mm thick was positioned at 30° to the beam, 14.1 cm from the target. Pulses from the detector were recorded using the TN1710 analyzer gated on the elastic triton peak.

3.2 Triton Source

The source used is a General Ionex model 830 sputter ion source modified for use with twelve cones as well as a second modification allowing it to be used for tritium. There were five tritiated titanium cones used with 100 Ci activity each. As well there were two test cones of hydrogenated titanium.

Tritium is an isotope of hydrogen which decays through β-emission to $^{3}He(T_{1/2}= 12.26$ years). The maximum β energy is very small at 18.6 keV so the β-particles are not an external radiation hazard. It is the possible incorporation of tritium into the body that provides the major hazard.

In the source, the primary release of tritium is due to sputtering during source operation. Contamination of the accelerator's beam system was minimized

by providing as much pumping restriction as possible, as well as adding to the source pumping system two additional titanium getter pumps. The average currents obtained out of the source were of the order of 600 nA with 150 nA analyzed at the target.

3.3 Target Preparation

The oxides of the target materials were purchased from the Isotope Sales Division of the Oak Ridge National Laboratory. The isotopic compositions as stated by the supplier are listed in table 1.

Samarium and ytterbium oxides were reduced using a procedure developed by Westgaard and Bjørnholm (1966) using lanthanum and thorium respectively as the reducing agents. The hafnium oxide was reduced using magnesium in a special procedure developed by Y. Peng. All three targets were prepared using a boat type evaporation onto carbon backings of approximately 40 $\mu g/cm^2$ thickness. A more complete description of the methods of preparing targets is given in appendix A.

3.4 Enge Spectrograph

The beauty in using this instrument is that it has a large solid angle of acceptance as well as high resolution, thus facilitating the study of reactions with relatively small cross-sections. The spectrograph is also designed to correct for kinematic broadening which occurs for large acceptance angles in the horizontal plane.

The instrument uses two-directional focussing and at the same time second-order focussing to maintain resolving power while increasing the solid angle of acceptance. The split between the poles of the magnet allows for vertical

TABLE 1

Percentage Abundance of Isotopes Contained in Targets

^{178}Hf		^{176}Yb		^{151}Sm	
174	0.05%	168	0.01%	147	0.937%
176	0.22	170	0.05	148	0.041
177	1.54	171	0.32	149	0.166
178	94.72	172	0.52	150	3.090
179	1.84	173	0.56	151	93.11 (86.50)*
180	1.69	174	2.12	152	2.390
		176	96.43	154	0.263

*Bracketed value is the adjusted value due to decay of ^{151}Sm.

focussing for low and high momentum particles in the fringing field zones at the entrances to the first and second pole gaps respectively. The focussing in this direction is only first order;however,its purpose is to increase the collecting power of the instrument not to produce an exact image of the object. Second-order focussing corrections in the focal plane are accomplished by suitable choices of curvatures and positions of the pole pieces (Spencer and Enge 1967). Typical trajectories for particles in the Enge spectrograph are illustrated in fig. 1.

For a given specific residual nucleus the excitation energy of the nuclear levels has a one-to-one correspondence with the position of its peak on the photographic plate, the intensity of the peak being proportional to the population probability of the given level.

A problem incurred in most spectra is that of impurity peaks obscured in some cases a large part of the spectra. It is found that impurities of lighter masses have significantly different foci due to the fact that focussing depends on the recoil energy loss and hence the mass of the bombarded nucleus. This results in a broadened peak espcially in the case where the mass of the impurity nucleus is significantly different from that of the target. It is also found that these peaks will appear to move to higher excitation energies as the reaction angle is increased.

The resolution of peaks in the spectrum is affected by many factors. The main factors contributing to peak broadening are the "in-target" effects. There is an effect due to differential energy loss in the target as well as one due to straggling. Because the proton and triton have different $\frac{dE}{dx}$ curves, the variation in location of the target where the reaction takes place causes a variation in the energy of the outgoing reaction products. Since the energy

Figure 1

Typical particle trajectories through the Enge Spectrograph.

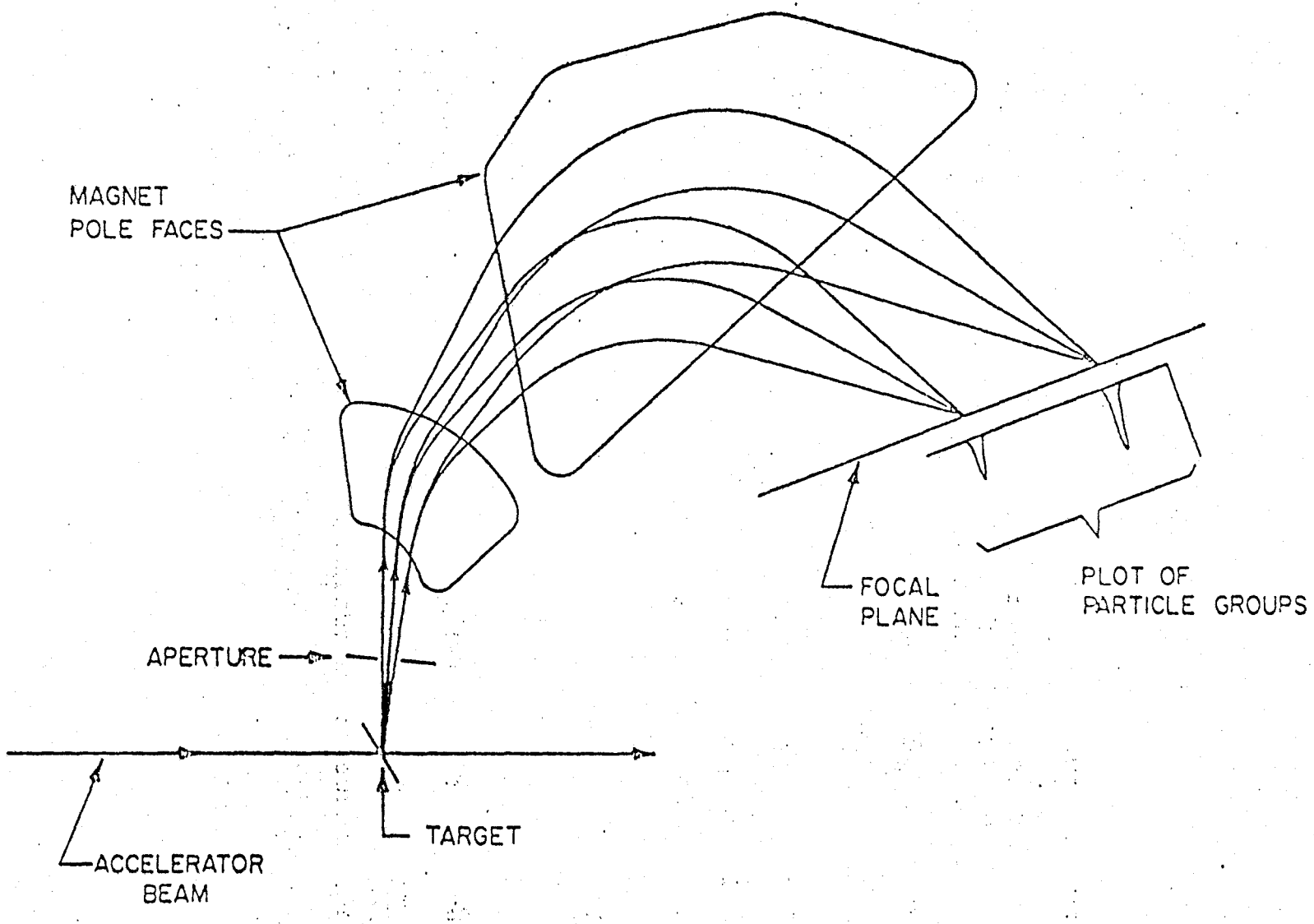
MAGNET
POLE FACES
APERTURE
ACCELERATOR
BEAM
TARGET
FOCAL
PLANE
PLOT OF
PARTICLE GROUPS

loss for a particle in traversing a given target material is also a statistical phenomenon, a spread in energy of the particles about their average energy is also expected (straggling).

Beam energy variations due to terminal instabilities have been estimated to account for about 1 keV width in the proton's peaks (Cairns 1979). As well, finite beam spot size on the target and the dispersion of magnets along the beam handling system also contribute to resolution losses. However the dispersion problem is partly compensated for by the dispersion of the spectrograph itself.

The total magnitude of all these effects has contributed to produce a FWHM value of about 15 keV in the spectra of this work.

CHAPTER IV

EXPERIMENTAL RESULTS

The number of counts collected in a detector in general is a product of the incoming flux of particles, the solid angle of acceptance of the detector, the thickness of the target and the cross-section involved in the reaction. Thus one has the relation;

$$N = \bar{\Phi}_{Incoming} \times (d\Omega)(t)\left(\frac{d\sigma}{d\Omega}\right)$$

where

$$\bar{\Phi}_I = \frac{Q(coul)}{1.6\times10^{-19}\,coul/triton} \quad \text{for this experiment.}$$

Since this relation holds true for both the monitor and the Enge spectrograph, by taking the ratio of N_{SPECT} to N_{MON} and rearranging it, one obtains the formula used to calculate absolute cross-sections,

$$\left(\frac{d\sigma}{d\Omega}\right)_{SPECT} = \left(\frac{d\sigma}{d\Omega}\right)_{MON} \times \frac{\Delta\Omega_{MON}}{\Delta\Omega_{SPECT}} \times \frac{N_{SP}}{N_{MON}} \times \frac{100\%}{\text{isotopic \%}}$$

The formula is corrected for isotopic compositions, as the first formula above assumed a pure target of a given material.

The elastic scattering cross-sections were calculated by the DWBA computer program DWUCK4(Kunz 1974) for the Sm, Yb and Hf targets. Values were calculated to be 4780 mb/sr, 5220 mb/sr and 6690 mb/sr respectively. These values are approximately 100% of the Rutherford cross-sections. The accuracy of the experimental absolute cross-sections using this method is about 20% for the stronger peaks. The relative cross-sections for a particular peak at different angles have an estimated accuracy of 10%.

Kodak NTB-50 nuclear emulsions were used to record the proton spectra for

these experiments. The photographic plates were covered with 0.25 mm Pb absorbers in order to remove any unwanted particles resulting from reactions in the target. As well the absorbers slow down the protons, causing an increased energy loss in the emulsion, thereby producing more distinct tracks. For all three nuclei under study, measurements were made at 9 angles ranging from $\theta_{LAB} = 7°$ to $\theta_{LAB} = 67.5°$. As well, interspersed at regular intervals were elastic short exposures taken at $\theta_{LAB} = 30°$. These were used as a check on the normalization values used for calculation of absolute cross-sections.

The raw data were reduced using the computer program SPECTR (O'Neil 1970) which fits the experimental peaks to a gaussian shape with an exponential tail. A set of adjustable parameters allowed the experimenter to vary the size and shape of the sample peak the computer chose. The program obtained the centroids for these peaks, then performed a laboratory to centre of mass kinematics calculation extracting the excitation energies and absolute cross-sections of the fitted peaks.

The energies and positions of the centroids of the peaks were cross-checked using programs constructed for the HP67 calculator. Peak yields were also double checked by summing by hand the total counts in the peak. Agreement was found to be at worst 5% for smaller peaks and less than 1% for the larger ones. Several spectra were recounted for the purpose of determining the reproducibility of the results as well as the accuracy of the counting microscopes and scanning personnel. Agreement in all cases was better than 1%. Energies and cross-sections for ^{153}Sm are shown in table 2.

The sample $^{151}Sm(t,p)^{153}Sm$ spectrum shown in fig. 2 is for $\theta_{LAB} = 60°$. At this angle most of the major peaks due to lighter impurities such as carbon and oxygen have moved through the spectrum. As well the cross-sections for the

TABLE 2

STATES POPULATED IN THE $^{151}Sm(t,p)^{153}Sm$ REACTION

Excitation Energy (keV)	$\frac{d\sigma}{d\Omega}$ (μb/sr)*	Percentage of Total Observed L=0 Strength
183	64	31.7
370	22	10.5
450	96	45.9
1082	27	11.8

* Cross-sections are for $\theta=30^{\circ}$

Figure 2

Proton spectrum at a laboratory angle of 60° for the $^{151}Sm(t,p)^{153}Sm$ experiment.

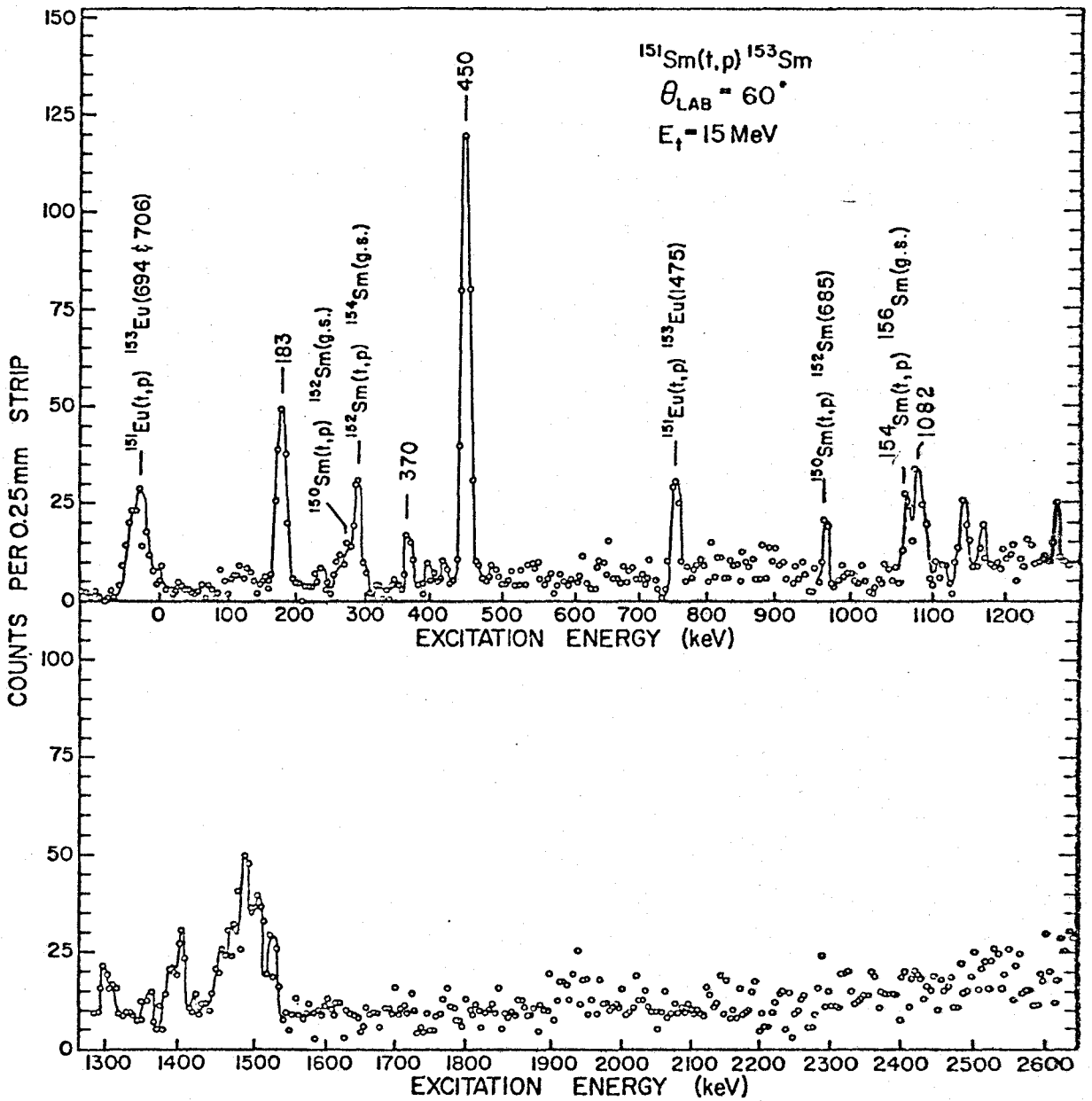
^{151}Sm(t,p)^{153}Sm
θ_{LAB} = 60°
E_t = 15 MeV
^{151}Eu(t,p) ^{153}Eu(694 & 706)
183
^{150}Sm(t,p) ^{152}Sm(g.s.)
^{152}Sm(t,p) ^{154}Sm(g.s.)
370
450
^{151}Eu(t,p) ^{153}Eu(1475)
^{150}Sm(t,p) ^{152}Sm(685)
^{154}Sm(t,p) ^{156}Sm(g.s.)
1082
COUNTS PER 0.25mm STRIP
EXCITATION ENERGY (keV)
EXCITATION ENERGY (keV)

remaining lighter impurities are reduced significantly at larger angles, whereas for peaks of interest in the heavier nuclei, $\theta=60°$ corresponds to a maximum in the L=0 transfer cross-section.

Clearly visible are the three major levels populated in the ^{153}Eu nucleus from the (t,p) reaction on the impurity ^{151}Eu. The ^{151}Eu contaminant is a result of β-decay of the target nucleus ^{151}Sm. The levels were identified using results obtained by Burke et al. (1975) on the reaction ^{151}Eu(t,p)^{153}Eu. Using the known ground state Q value of 6.373 ± .003 MeV (Wapstra and Bos 1977) for the above mentioned reaction, and the observed impurity peaks, a precise Q-value calibration was obtained for the spectra. Q-values for the ground states of various impurities are listed in table 3. This method of calibration proved to be very useful for the ^{153}Sm odd-even nucleus, as the Q-value for the ^{151}Sm(t,p)^{153}Sm reaction was known to be 5.644 ± 0.001 MeV (Wapstra and Bos 1977)(see table 3). It thus became possible to locate the position in the spectra where the ground state should be found to within an uncertainty of 3 keV.

Since the target was known to have also a substantial amount of the isotopic impurity ^{152}Sm the appearance of the ground state of ^{154}Sm due to the reaction ^{152}Sm(t,p)^{154}Sm at the correct proton energy location added further confidence to the calibration.

Angular distributions for the ^{153}Eu levels are shown in fig. 3. Due to a large number of impurity peaks at the forward angles only upper limits could be set on many of the cross-section values. The DWBA curves superimposed on the data points were calculated using the program DWUCK4. Optical triton and proton parameters used in this calculation were taken from Flynn et al. (1969).

Since the (t,p) reaction is highly selective, favouring states of the final nucleus which have a large parentage based on the ground state of the target

TABLE 3

GROUND STATE Q-VALUES FOR Sm and Eu ISOTOPES

	S(2n) (keV)*	Q(MeV)
^{150}Sm	13857.1(0.3)	5.375
^{151}Sm	13582.3(1.1)	5.100
^{152}Sm	13855.2(1.0)	5.373
^{153}Sm	14125.9(1.0)	5.644
^{154}Sm	13835.6(0.9)	5.354
^{156}Sm	13057.0(13.0)	4.575
^{153}Eu	14855.1(2.9)	6.373

*Taken from Wapstra and Bos (1977). Values in brackets are errors in keV.

Figure 3

Angular distributions for the 1475 keV level and the 694, 706 keV doublet for the $^{151}Eu(t,p)^{153}Eu$ reaction.

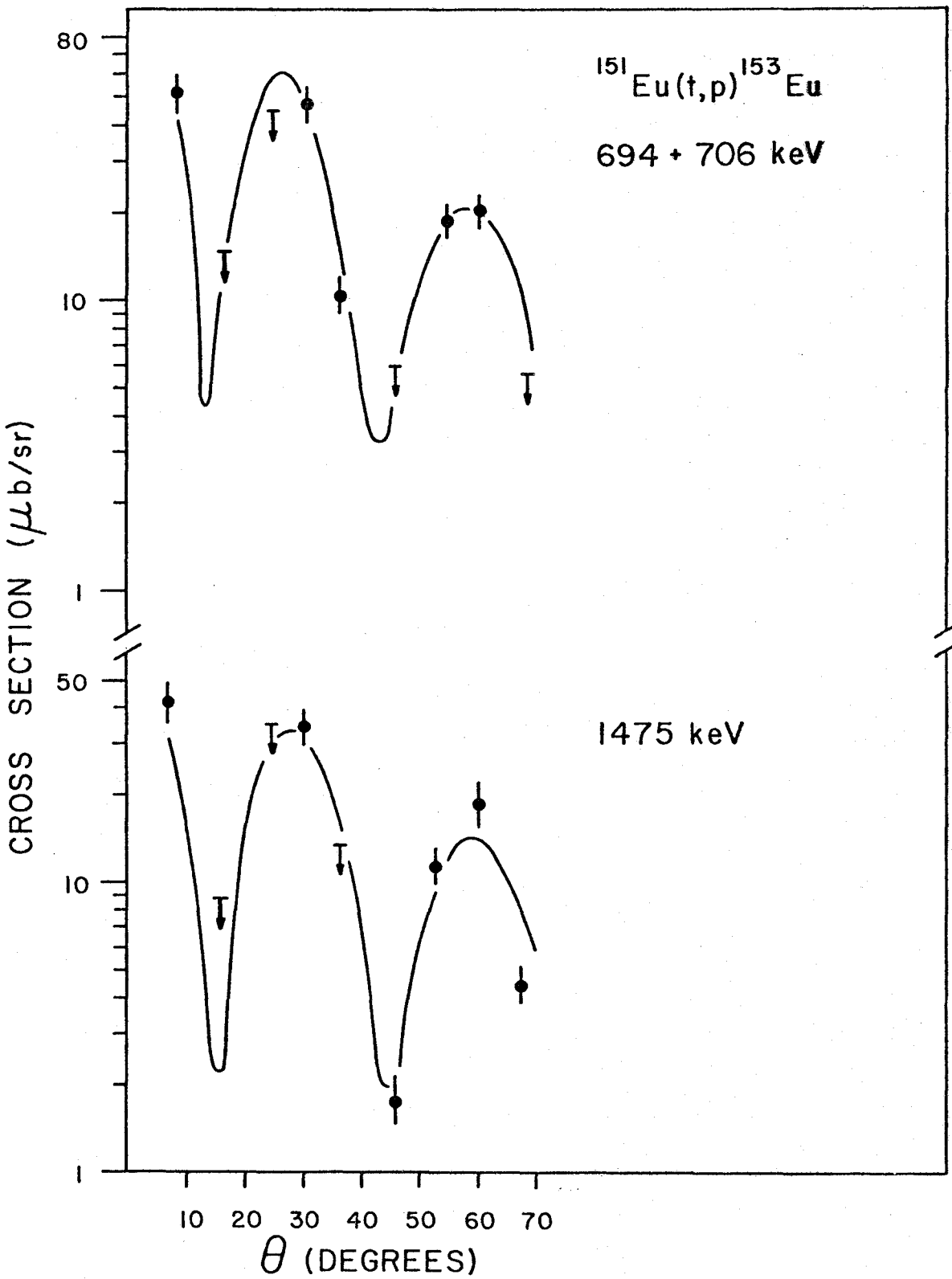
80
10
1
50
10
1
CROSS SECTION (μb/sr)
^{151}Eu(t,p)^{153}Eu
694 + 706 keV
1475 keV
10 20 30 40 50 60 70
θ (DEGREES)

nucleus, a search was made for states of $5/2^-$ spin and parity (the ground state assignment for the target nucleus ^{151}Sm (Robertson et al 1971, Nelson et al 1973)).

Using the Q value for the reaction $^{151}Sm(t,p)^{153}Sm$ and the calibration mentioned earlier, the previously known 183 keV and 450 keV levels in ^{153}Sm (Kenefick et al. 1965) were clearly identified. The angular distributions for these levels in fig. 4 show distinctive L=0 diffraction patterns. Clear maxima are visible at $\theta=30°$ and $\theta=60°$ with minima at 15° and 45°. Optical model parameters were once again taken from Flynn et al. (1969). The cross-sections are given in table 2. Also listed in table 2 are levels at 370 keV and 1082 keV which show the L=0 diffraction pattern. These angular distributions are illustrated in fig. 5. The 1064 keV peak labelled on the $\theta=60°$ ^{151}Sm spectrum (fig. 2) is believed to be the ground state of ^{156}Sm, populated in the reaction, $^{154}Sm(t,p)^{156}Sm$.

Figure 4

Angular distributions for the 183 and 450 keV levels in ^{153}Sm.

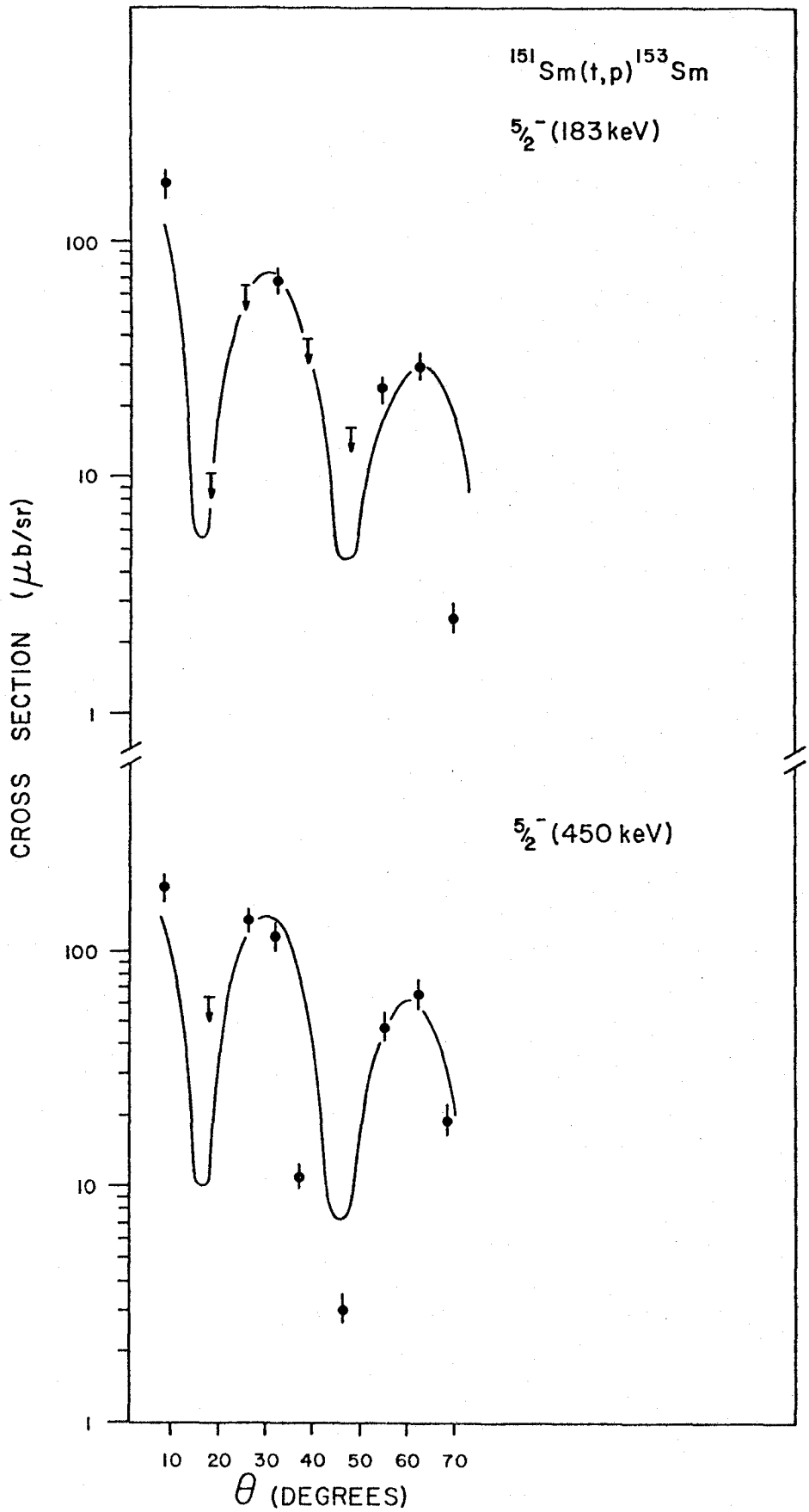
$^{151}Sm(t,p)^{153}Sm$
$5/2^-$ (183 keV)
$5/2^-$ (450 keV)
CROSS SECTION (μb/sr)
100
10
1
100
10
1
10 20 30 40 50 60 70
θ (DEGREES)

Figure 5

Angular distributions for the 370 and 1082 keV levels tentatively assigned to the ^{153}Sm nucleus.

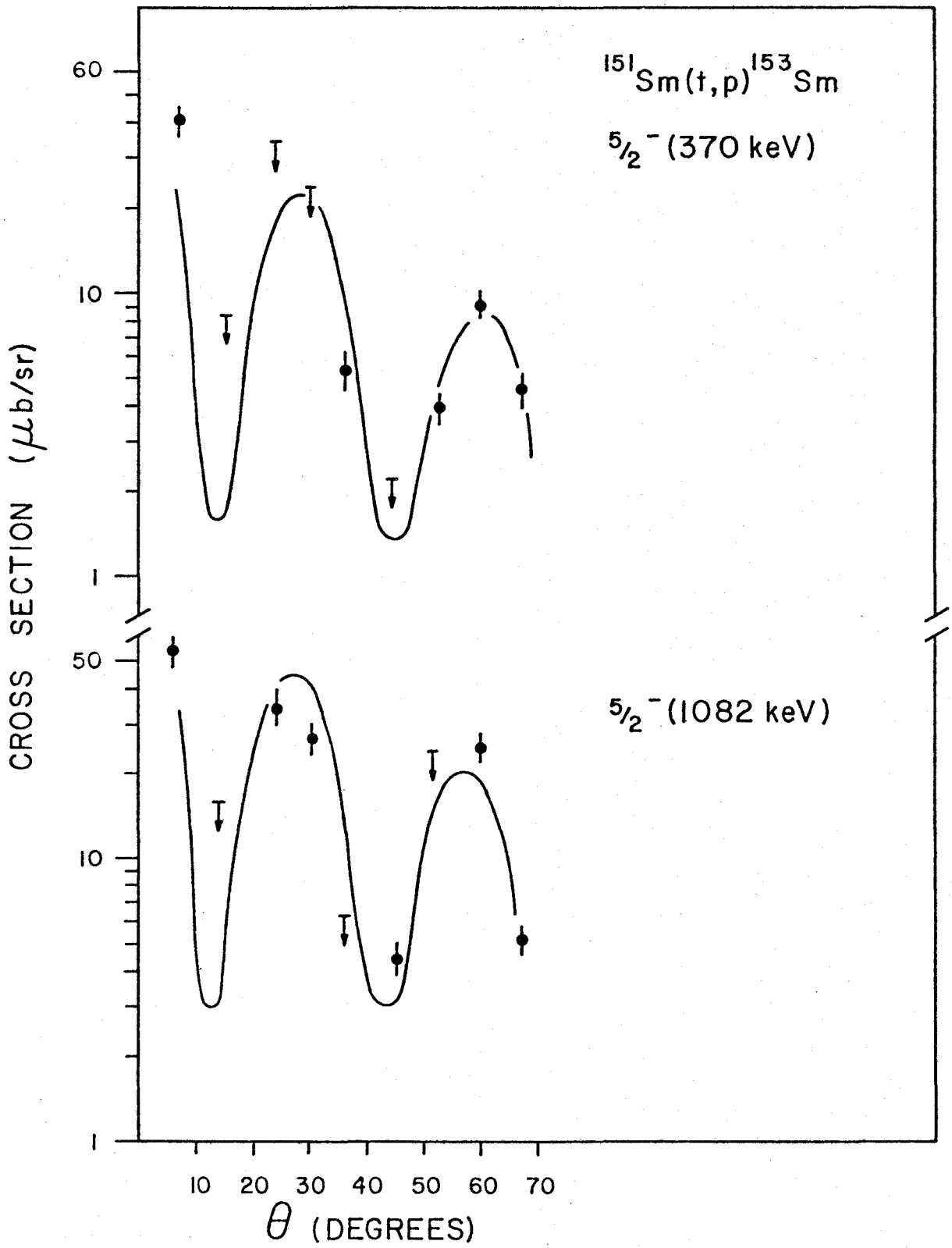
$^{151}Sm(t,p)^{153}Sm$
$5/2^-$ (370 keV)
$5/2^-$ (1082 keV)
CROSS SECTION (μb/sr)
60
10
1
50
10
1
10 20 30 40 50 60 70
θ (DEGREES)

CHAPTER V

DISCUSSION OF Sm RESULTS

The appearance of the 183 keV and 450 keV levels was predicted theoretically by two independent groups; Rekstad et al. (1978) and Katajanheimo and Hammaren (1978). Both groups have perfomed calculations on the target nucleus ^{151}Sm as well as the residual nucleus ^{153}Sm.

Rekstad et al. (1978) use a particle-rotor model where they have constructed a single-particle potential relevant for the ^{153}Sm nucleus from the observed level structure of this nucleus as well as explicitly treating the recoil term in the Hamiltonian. The details of their calculations are contained in a not yet published article on ^{153}Sm.

Katajanheimo and Hammaren (1978) use the particle-rotor model with a nonspheroidal axial and reflection symmetric Woods-Saxon potential. Spherical and well-deformed nuclei were used to find parameter systematics. The description of the particle-rotor model may be found in an article by Wahlborn et. al. (1966).

In table 4 the amplitudes of the Nilsson orbitals of the ground state of ^{151}Sm are listed as calculated by each group. Both groups agree that the ground state configuration is primarily composed of the $3/2^-[532]$ state and the $5/2^-[523]$ state. In tables 5 and 6 all calculated $5/2^-$ states in ^{153}Sm are listed with their corresponding Coriolis mixed amplitudes. Based on the ground state assignment in ^{151}Sm, those $5/2^-$ states in ^{153}Sm with strong admixtures of either of the two above mentioned Nilsson states would be expected to be seen experimentally.

Both groups' calculations indicate the presence of two levels, one at the

TABLE 4

CALCULATED NILSSON AMPLITUDES FOR ^{151}Sm GROUND STATE

	$1/2^-[521]$	$5/2^-[523]$	$3/2^-[521]$	$3/2^-[532]$	$11/2^-[505]$	$1/2^-[530]$
ekstad et al. (1978)	0.07	0.32	-0.14	0.92	0	0.16
ammaren (1978)	0.06	-0.61	-0.05	0.78	0	-0.04

TABLE 5

CALCULATED $5/2^-$ STATES IN ^{153}Sm by KATAJANHEIMO AND HAMMAREN (1978)

Calc. E_x (keV)	Amplitudes of Nilsson orbitals in wavefunctions							
	$1/2^-[541]$	$1/2^-[530]$	$1/2^-[521]$	$1/2^-[510]$	$3/2^-[532]$	$3/2^-[521]$	$5/2^-[523]$	$5/2^-[512]$
91.1	0.005	0.133	0.001	0.013	0.030	-0.990	-0.001	0.046
210.0	0.040	0.048	0.054	0.000	-0.990	-0.023	0.111	0.007
615.0	-0.040	-0.981	-0.111	0.013	-0.044	-0.133	0.066	0.009
656.0	-0.003	0.061	-0.009	0.001	0.113	0.010	0.992	-0.015
891.0	0.039	0.110	-0.991	-0.034	-0.048	0.012	-0.010	-0.000
1524.0	-0.001	0.004	0.000	-0.002	0.008	0.047	0.014	0.999

TABLE 6

CALCULATED $5/2^-$ STATES IN ^{153}Sm by REKSTAD *et al.*

Calc. E_x (keV)	Amplitudes of Nilsson orbitals in wavefunction						
	$9/2^-[514]$	$1/2^-[530]$	$3/2^-[532]$	$11/2^-[505]$	$3/2^-[521]$	$5/2^-[523]$	$1/2^-[521]$
88	0	0.08	0.04	0	0.99	0.01	-0.04
187	0	0	1.00	0	-0.04	0.06	0.04
452	0	-0.01	-0.06	0	-0.01	1.00	0.01
487	0	0.99	0	0	-0.08	0.01	-0.05
796	0	0.06	-0.04	0	0.04	-0.01	1.00

observed energy of 183 keV (corresponding to a calculated value of 187 keV for Rekstad et al. (1978) and 210 keV for Katajanheimo and Hammaren (1978)) and one with a strong $5/2^-[523]$ component with no corresponding experimentally observed level listed (level has a calculated value of 452 keV for Rekstad et al. (1978), and 656 keV for Katajanheimo and Hammaren (1978)).

However the experimentally known 450 keV level has been tentatively assigned by both groups as the $5/2^-$ member of the $1/2^-[530]$ band. Based on this assignment, the 450 keV level would not be expected to be strongly populated by the (t,p) reaction. The origin of the $5/2$, $1/2^-[530]$ assignment stems back to the work of Bennett et al. (1971). Based upon the results of Tjøm and Elbek on the odd mass Gd nuclei which suggested that the $5/2^-$ member of the $1/2^-[530]$ band could reasonably occur 30-40 keV above the $3/2^-$ member, Bennett et al. (1971) assigned the previously seen 450 keV level to this band. The $3/2^-$ member was observed at 405 keV using the $^{154}Sm(d,t)^{153}Sm$ reaction. The suggested $5/2^-$ member at 450 keV level was not observed and was believed to be obscured by the strongly populated $7/2^+$ state at 447 keV. The whole band assignment has been listed as tentative and has remained so until the present day.

Listed in table 7 are the Nilsson wave functions for ^{151}Sm and ^{153}Sm from the work of Rekstad et al. (1978). The wavefunctions for the Hammaren (1978) group are included in Table 8. It is seen that the wavefunctions for the $5/2^-[523]$ and the $3/2^-[532]$ Nilsson states do not change significantly between the ^{151}Sm and ^{153}Sm nuclei. Thus it is possible to calculate approximately relative intensities for the transitions to the two levels as;

$$\frac{d\sigma}{d\Omega} \propto \left| \sum_i a^i_{g.s.} \, a^i_{final} \right|^2$$

where $a^i_{g.s}$ is the Coriolis mixed coefficient for the ground state of ^{151}Sm, and a^i_f is the coefficient for the final nucleus.

TABLE 7

AMPLITUDES OF ANGULAR MOMENTUM j IN NILSSON ORBITALS

FOR ^{151}Sm and ^{153}Sm (REKSTAD et al.)

C_j^{ℓ}	$1/2^-[521]$	$5/2^-[523]$	$3/2^-[521]$	$3/2^-[532]$	$11/2^-[505]$	$1/2^-[530]$	$9/2^-[514]$
j = 1/2	-0.45(0.46)	0(0)	0(0)	0(0)	0(0)	0.10(0.09)	0(0)
3/2	0.35(-0.32)	0(0)	0.13(0.15)	0.29(0.29)	0(0)	0.29(0.31)	0(0)
5/2	0.20(0.22)	0.20(0.23)	-0.28(-0.27)	0.40(0.42)	0(0)	-0.45(-0.45)	0(0)
7/2	0.53(-0.52)	-0.85(-0.81)	-0.56(-0.58)	-0.65(-0.62)	0(0)	-0.51(-0.51)	0(0)
9/2	0.57(-0.58)	-0.42(-.047)	0.76(0.74)	-0.44(-0.46)	0(0)	0.61(0.60)	-0.03(-0.04)
11/2	0.16(-0.16)	-0.24(-0.26)	-0.12(-0.14)	-0.37(-0.38)	1.00(1.00)	-0.26(-0.28)	1.00(1.00)

*Bracketed values are for ^{153}Sm

TABLE 8

*SINGLE-PARTICLE WAVEFUNCTIONS FROM THE CALCULATION WITH THE WOODS-SAXON POTENTIAL (HAMMAREN 1978)

		$3/2^-[321]$	$3/2^-[541]$	$3/2^-[532]$	$3/2^-[521]$	$3/2^-[512]$	$3/2^-[501]$
^{151}Sm	$3/2^-[532]$	0.1	0.69	0.29	-0.48	0.40	-0.20
^{153}Sm	$3/2^-[532]$	-0.08	0.55	0.70	-0.32	0.27	-0.09

		$5/2^-[312]$	$5/2^-[532]$	$5/2^-[523]$	$5/2^-[512]$	$5/2^-[503]$
^{151}Sm	$5/2^-[523]$	-0.1	0.52	0.30	-0.73	0.30
^{153}Sm	$5/2^-[523]$	-0.07	0.45	0.70	-0.50	0.20

*The components shown are those of cylindrical representation. Overlap between the single-particle states was calculated to be 0.85 and 0.88 for the $3/2^-[532]$ and $5/2^-[532]$ collective states respectively.

Both groups' results predict that the L=0 strength of the 183 keV level should be larger than that of the 450 keV level (by a factor of 2.6 for Hammaren (1978) and 12.8 for Rekstad et al. (1978)). However it was observed experimentally that the 450 keV peak contained approximately 1.5 times the L=0 strength of the 183 peak.

As mentioned earlier two states at 370 keV and 1082 keV were observed to have L=0 angular distributions. The levels do not correspond to any previously reported $5/2^-$ states in ^{153}Sm nor any levels predicted by the two calculations mentioned in this study. The absence of any systematic shift in excitation energy with angle for the two levels indicates that they belong to a nucleus with mass 153±2 mass units, however a search for possible impurities was unsuccessful. Thus they have been tentatively assigned as $5/2^-$ states in ^{153}Sm.

It is a surprising observation that the sum of the L=0 strength in the $^{151}Sm(t,p)^{153}Sm$ reaction below 2 MeV excitation energy amounts to about 50% of that observed with the $^{151}Eu(t,p)^{153}Eu$ and $^{153}Eu(t,p)^{155}Eu$ reactions (Burke et al. 1975). As well the total L=0 strength is down considerably from values obtained in the reactions on the even isotopes of Sm (Bjerregaard et al. 1966). A further scan up to 3 MeV did not reveal any major peaks as illustrated by the representative θ=60°, ^{153}Sm spectrum. It is possible that the L=0 strength is fragmented over many levels, each with a small cross-section such that the peaks cannot be observed above the background in the spectrum. It would also be expected that the total cross-section would be reduced by blocking effects of the odd neutron. However the blocking by an $I^\pi = 5/2^-$ neutron would not be expected to have such a large effect. It is most likely that both of these factors are contributing.

CHAPTER VI

SUMMARY AND CONCLUSIONS OF Sm DATA

In the $^{151}Sm(t,p)^{153}Sm$ reaction it was found that the total L=0 strength was spread over at least 4 levels. The two previously reported levels at 183 keV and 450 keV contained 77% of the total L=0 strength. The 370 keV and 1082 keV levels have been tentatively assigned as $5/2^-$ state in ^{153}Sm.

Calculations performed on ^{151}Sm and ^{153}Sm by Katajanheimo and Hammaren (1978) and Rekstad et. al. (1978) predicted two levels to be preferentially populated. According to the interpretations of both groups the 183 keV level should have the largest cross-section as it was assigned as a $3/2^-[532]$ neutron state, which is the major component of the ^{151}Sm ground state (according to both groups' calculations). However, experimental results indicate that the cross-section for the 183 keV level corresponds to only $\sim$ 30% of the total observed L=0 strength which in turn is only about half as large as the cross-sections seen in the neighbouring nuclei.

The predictions of Rekstad et. al. (1978) though not appearing to be as close in agreement with these experimental results as Katajanheimo and Hammaren's (1978) calculations still have very impressive agreement to a large body of single-nucleon transfer, Coulomb excitation and gamma decay data. The wavefunctions of Katajanheimo and Hammaren (1978) were not in a form amenable for the calculation of single-nucleon transfer cross-sections and hence data of this type were not considered in optimizing the fit. Rekstad also feels that the wavefunctions can most likely be altered to reproduce the relative strengths of the 183 and 450 keV levels in the experiment without altering significantly the overall agreement achieved in explaining the other properties of the nuclei (Rekstad 1978).

CHAPTER VII

DISCUSSION OF ^{178}Yb AND ^{180}Hf RESULTS

The transfer of two neutrons from an even-even rare earth nucleus in general leads to a strong ground-state to ground-state transition, which contains most of the transferred L=0 strength. It is found that the ground states of rare earth nuclei are dominated by pairing collectivity. This same collectivity is responsible for the strong two-nucleon transfer transitions.

However there are cases where fragmentation of the pairing strength occurs which leads to the existence of excited 0^+ states carrying a large percentage of the L=0 strength. This fragmentation is attributed to an energy gap in the single particle spectrum which partially decouples the levels above the gap from the levels below the gap. Such a gap is found at neutron number N=108 and is seen to clearly show up if one looked at the two-neutron separation energies for the Hf and Yb nuclei (Wapstra & Bos 1977). The general downward trend of the curves for increasing mass is broken at N=108 where one encounters a larger than average energy spacing. This is illustrated in fig. 6. As well fig. 7 shows the corresponding energy gap above the $9/2^+[624]$ orbital in the Nilsson scheme.

The representative spectra for ^{178}Yb and ^{180}Hf given in figs. 8 and 9 show the strongly excited 0^+ state having approximately 60% of the ground state strength. Listed in table 9 are the energies of the levels indicated on the spectra and the corresponding cross-sections for the 0^+ states. The angular distributions for these states are given in figs. 10 and 11. Optical model parameters used for the DWBA curves were taken from Flynn *et al.* (1969). In both cases the ground state rotational band is seen up to the 4^+ member and in some angles up to the 6^+ member. The values of $\frac{\hbar^2}{2\mathcal{I}}$ were calculated to be

Figure 6

The two-neutron separation energies for the various Hf isotopes. The parallel lines are to emphasize the discontinuity at N=108.

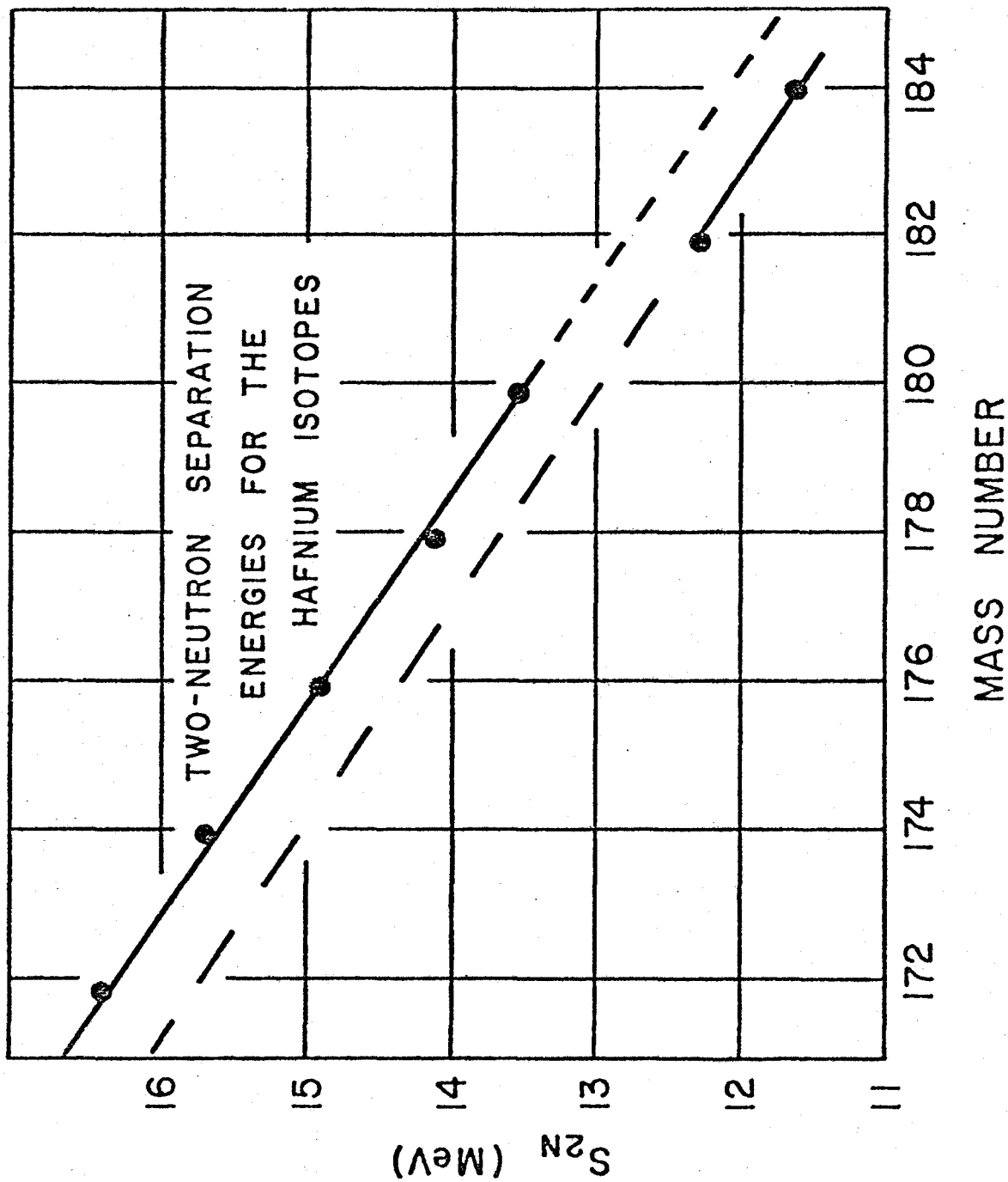
TWO-NEUTRON SEPARATION ENERGIES FOR THE HAFNIUM ISOTOPES
S_{2N} (MeV)
16
15
14
13
12
11
172
174
176
178
180
182
184
MASS NUMBER

Figure 7

Nilsson diagram for neutron orbitals.

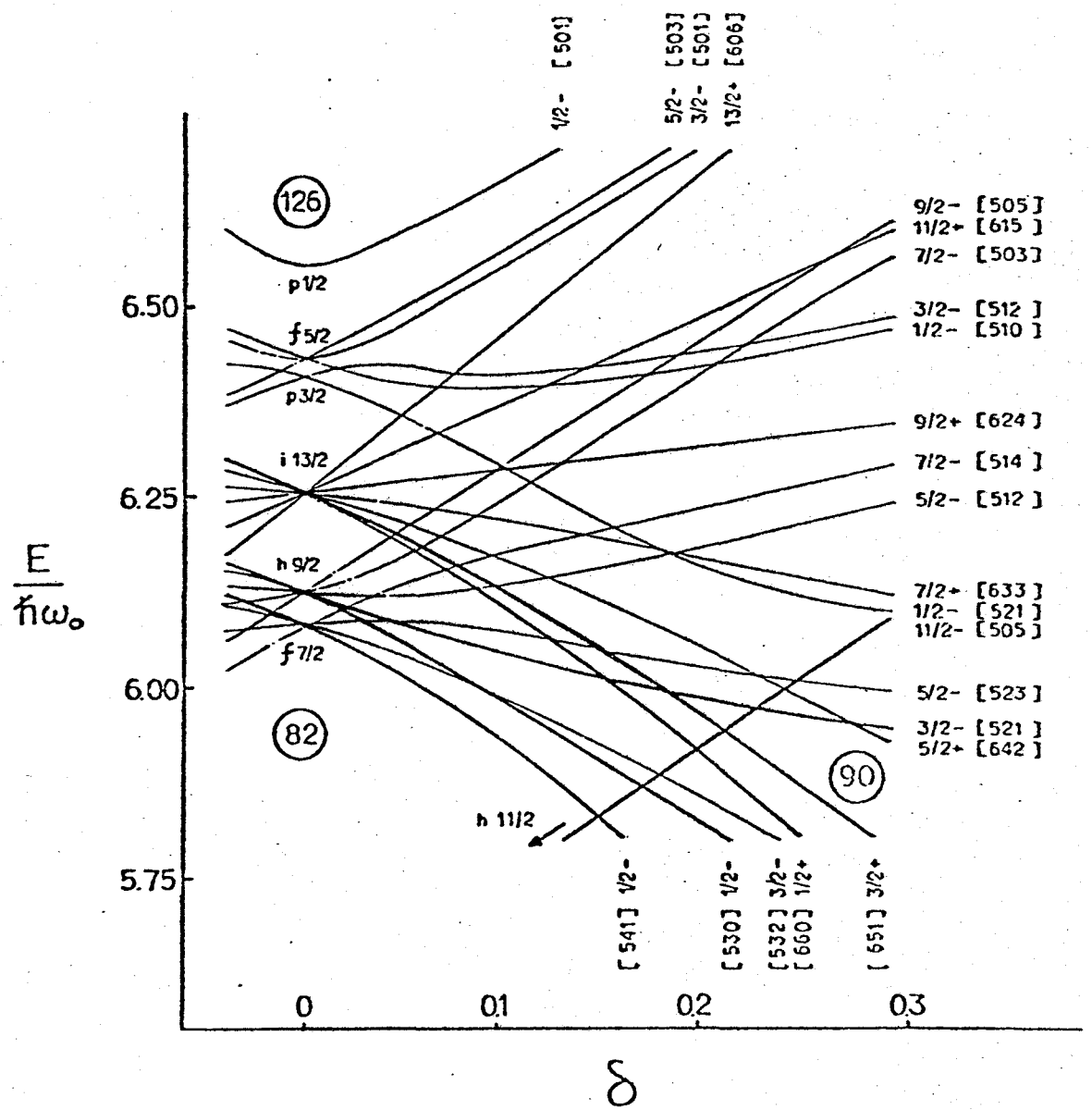
1/2- [501]
5/2- [503]
3/2- [501]
13/2+ [606]
126
p1/2
f5/2
p3/2
i13/2
h9/2
f7/2
82
h11/2
9/2- [505]
11/2+ [615]
7/2- [503]
3/2- [512]
1/2- [510]
9/2+ [624]
7/2- [514]
5/2- [512]
7/2+ [633]
1/2- [521]
11/2- [505]
5/2- [523]
3/2- [521]
5/2+ [642]
90
[541] 1/2-
[530] 1/2-
[532] 3/2-
[660] 1/2+
[651] 3/2+
6.50
6.25
6.00
5.75
E/ħω₀
0
0.1
0.2
0.3
δ

Figure 8

Proton spectrum at a laboratory angle of 60° for the $^{178}Hf(t,p)^{180}Hf$ experiment.

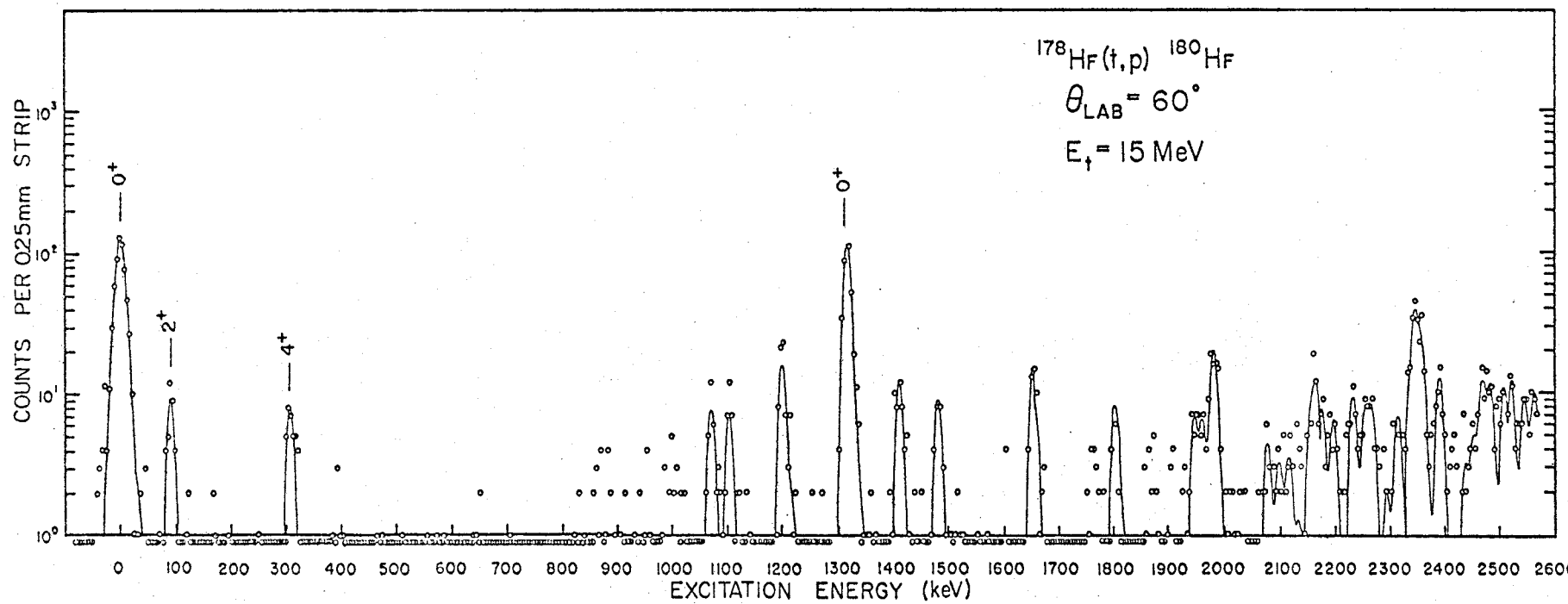
^{178}Hf(t,p) ^{180}Hf
θ_{LAB} = 60°
E_t = 15 MeV
0+
2+
4+
0+
COUNTS PER 0.25mm STRIP
10^3
10^2
10^1
10^0
0 100 200 300 400 500 600 700 800 900 1000 1100 1200 1300 1400 1500 1600 1700 1800 1900 2000 2100 2200 2300 2400 2500 2600
EXCITATION ENERGY (keV)

Figure 9

Proton spectrum at a laboratory angle of 60° for the $^{176}Yb(t,p)^{178}Yb$ experiment.

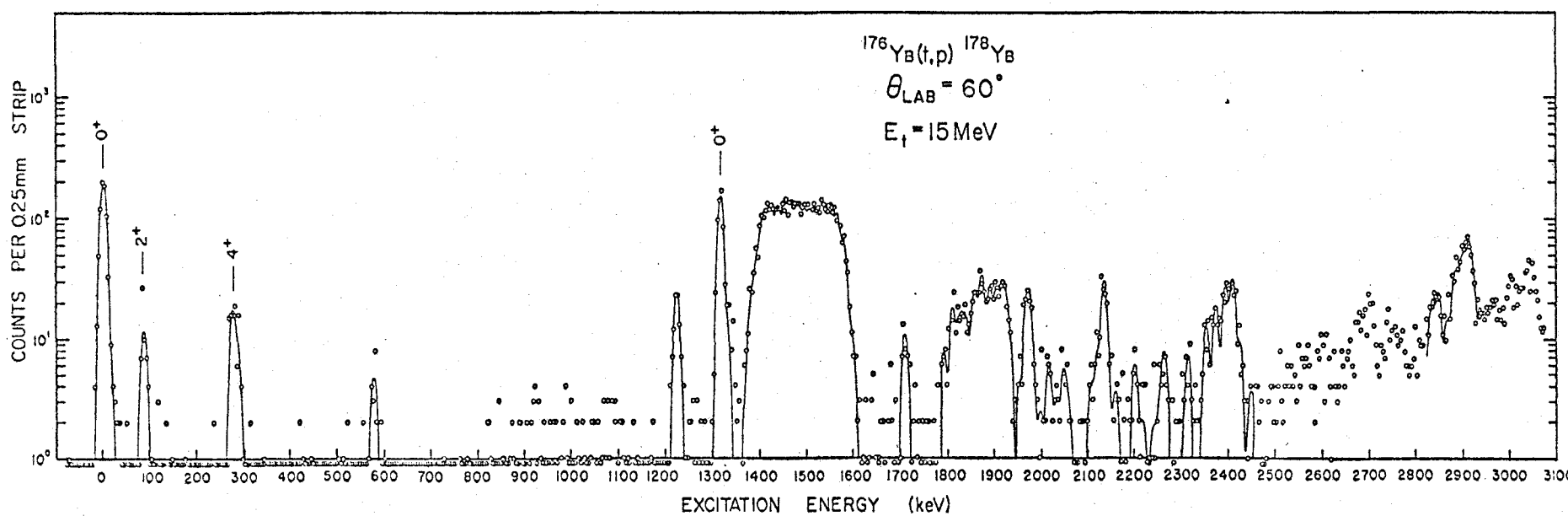
^{176}Yb(t,p) ^{178}Yb
θ_{LAB} = 60°
E_t = 15 MeV
0+
2+
4+
0+
COUNTS PER 0.25mm STRIP
EXCITATION ENERGY (keV)

TABLE 9

STATES POPULATED IN THE REACTION $^{178}Hf(t,p)^{180}Hf$

Excitation Energy (keV)	I^{π}	$\frac{d\sigma}{d\Omega}$(μb/sr)*	Percentage of Total observed L=0 Strength
g.s.	0^+	93	58.3
93	2^+		
308	4^+		
641	6^+		
1317	0^+_1	70	41.7

STATES POPULATED IN THE REACTION $^{176}Yb(t,p)^{178}Yb$

g.s.	0^+	98	57.8
83	2^+		
275	4^+		
1311	0^+_1	72	42.2

* Cross-sections are for θ=30°.

Figure 10

Angular distributions for the ground state and first excited 0^+ state in ^{180}Hf.

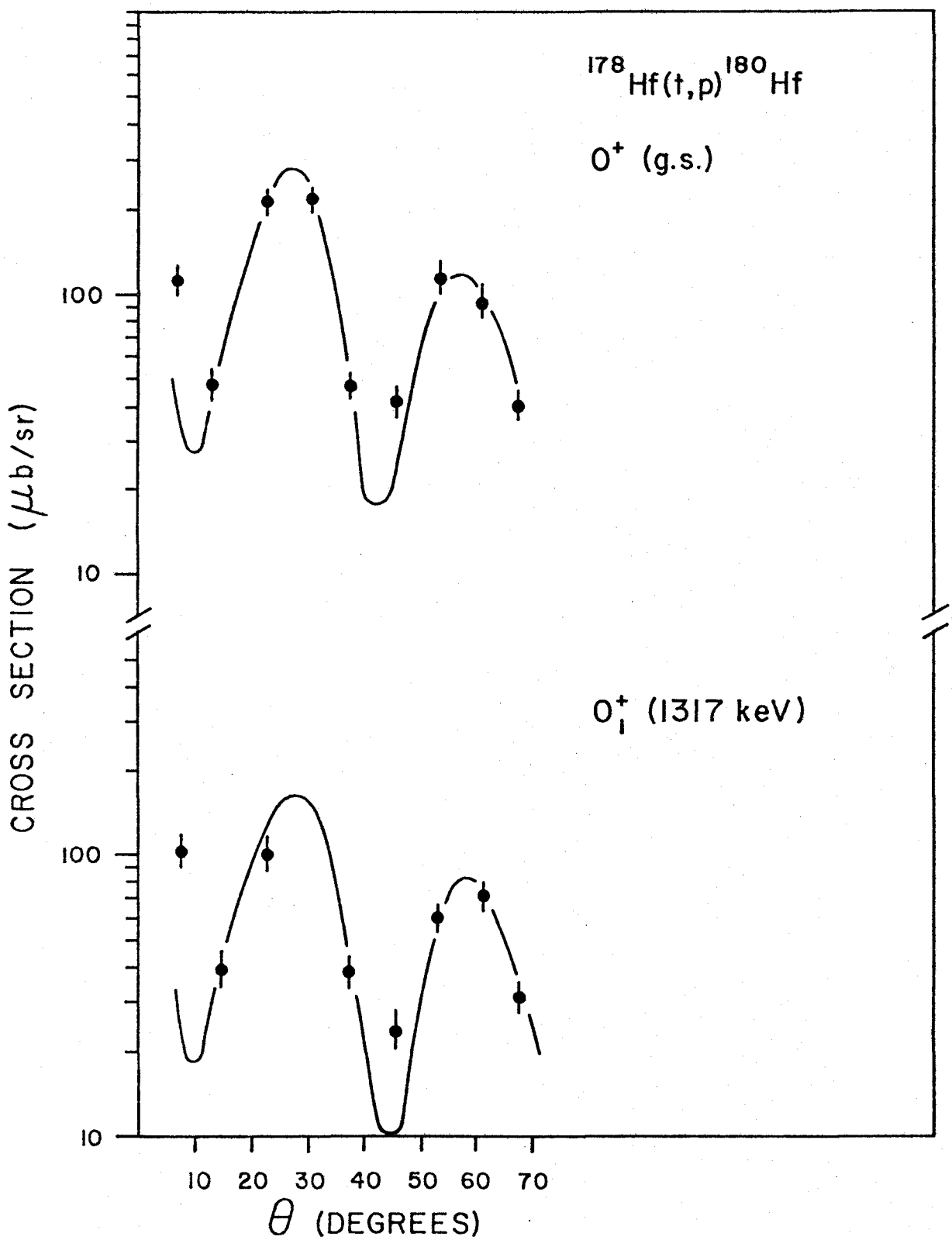
^{178}Hf(t,p)^{180}Hf
0^+ (g.s.)
0^+_1 (1317 keV)
CROSS SECTION (μb/sr)
100
10
100
10
10 20 30 40 50 60 70
θ (DEGREES)

Figure 11

Angular distributions for the ground state and first excited 0^+ state in ^{178}Yb.

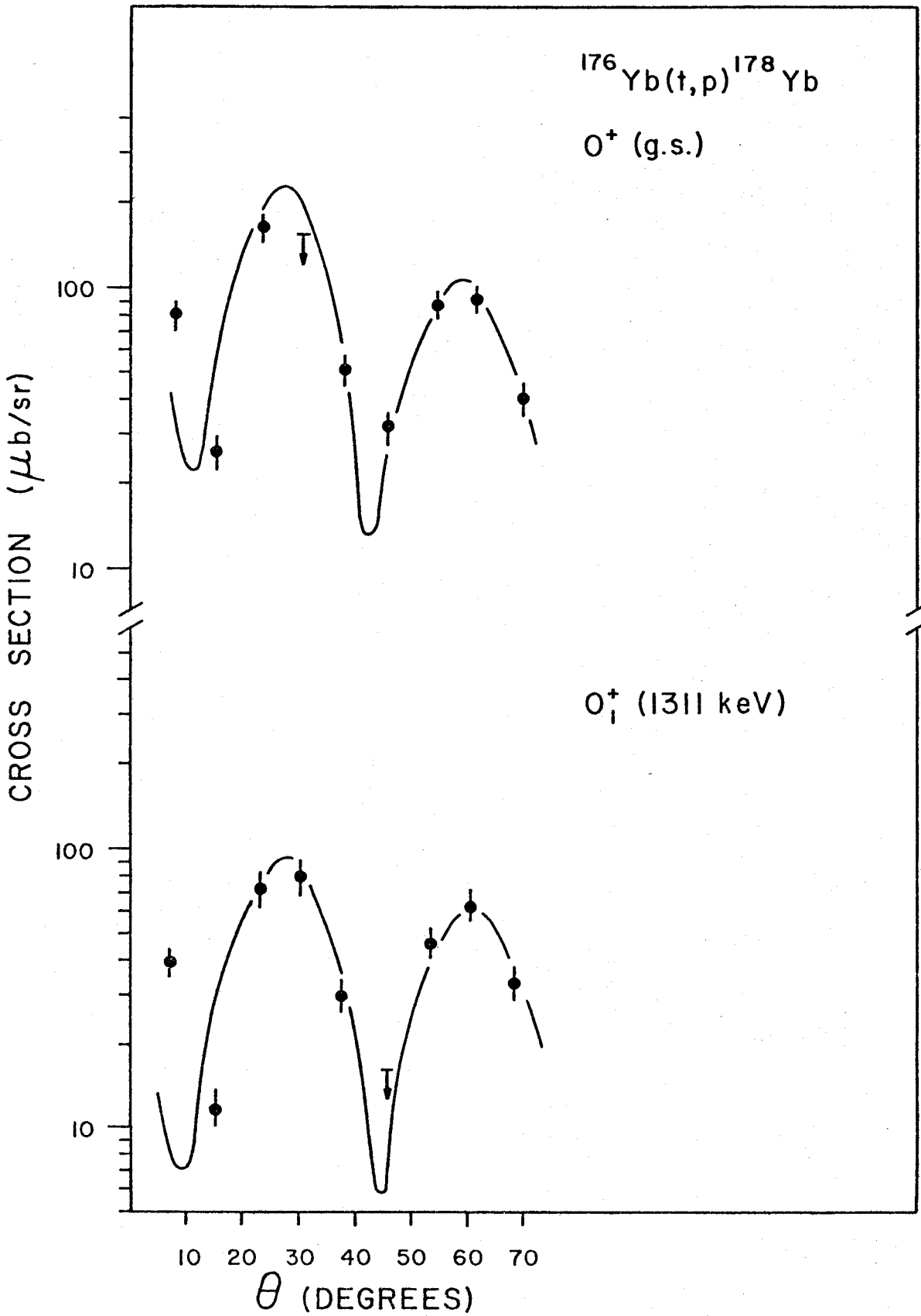
^{176}Yb(t,p)^{178}Yb
0^+ (g.s.)
0^+_1 (1311 keV)
CROSS SECTION (μb/sr)
100
10
100
10
10 20 30 40 50 60 70
θ (DEGREES)

15.55 keV and 13.83 keV for ^{180}Hf and ^{178}Yb respectively.

Mortensen (1978) in a thesis published shortly after these results were obtained observes the same phenomenon in the isotone ^{182}W using the reaction ^{180}W(t,p)^{182}W. The excited 0^+ state in ^{182}W contained 40% of the ground state 0^+ strength.

At present no one theory adequately describes the observed strongly excited 0^+ states. The B.C.S. theory is found to breakdown in places where there exists an energy gap in the level spacings.

Mortensen (1978) in his study gives the shapes of Fermi surfaces for the even-even W isotpes. Illustrated in fig. 12 is a sample of his calculations showing a situation where B.C.S. theory is appropriate as well as the ^{182}W case where the orbitals above the gap are almost completely empty and the orbits below the gap almost full. As well the gap energy is of the order of the pairing energy for this nucleus. On this criterion he suggests the pairing-vibration model of Bès and Broglia (1966) might be considered.

In this model the ground state of the nucleus is taken to be the vacuum state where $N=N_o$. The 0^+ states are then created by using defined creation and annihilation operators which either add two neutrons or remove two neutrons below the gap. Fig. 13 illustrates the predictions of the model where the notation labelling a state is (N_r,N_a); N_r is the number of removal quanta and N_a is the number of addition quanta needed to form the state from the vacuum. This figure shows that not only the existence of certain states but also their relative strengths are predicted. Thus the (0,2) state has twice the strength of the (0,1) state, as formed in the (t,p) reaction.

However the model manages to predict only the states expected to be strongly (or weakly) populated in (t,p) or (p,t) reactions. The agreement between experiment and model for relative energies and intensities is found to be very

Figure 12

Shapes of the Fermi surfaces are given for each of the even-mass W isotopes. Calculations were performed within the framework of the B.C.S. theory.

The fact that in ^{182}W the orbitals above the gap are almost completely empty and the orbitals below the gap almost completely full suggests the applicability of the pairing vibration model. Figure is taken from Mortensen (1978).

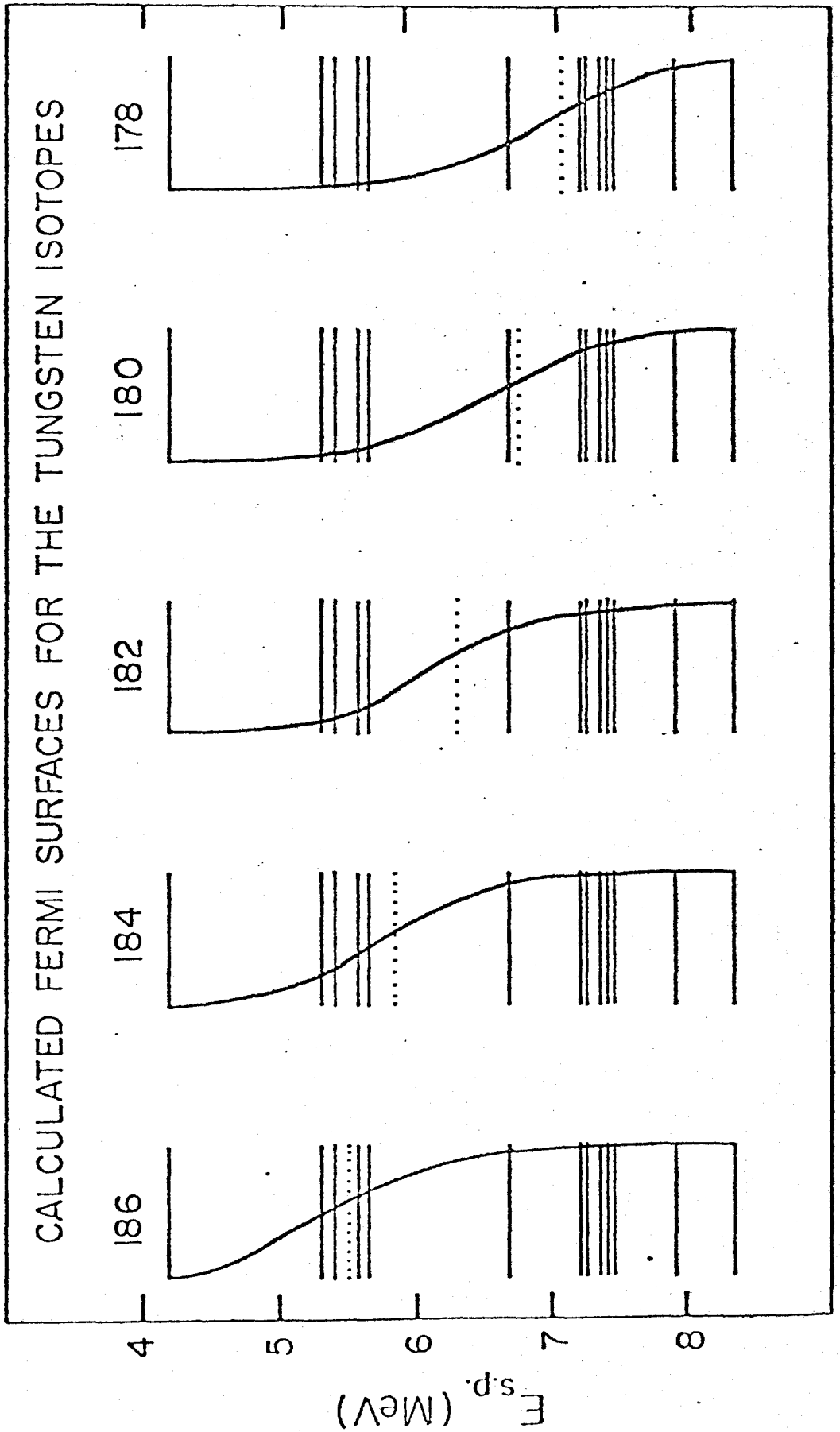
CALCULATED FERMI SURFACES FOR THE TUNGSTEN ISOTOPES
178
180
182
184
186
4
5
6
7
8
$E_{s.p.}$ (MeV)

Figure 13

The predictions of the harmonic pairing vibration theory for the relative energies of 0^+ states and for the (t,p) and (p,t) cross-sections. Figure is taken from Mortensen (1978).

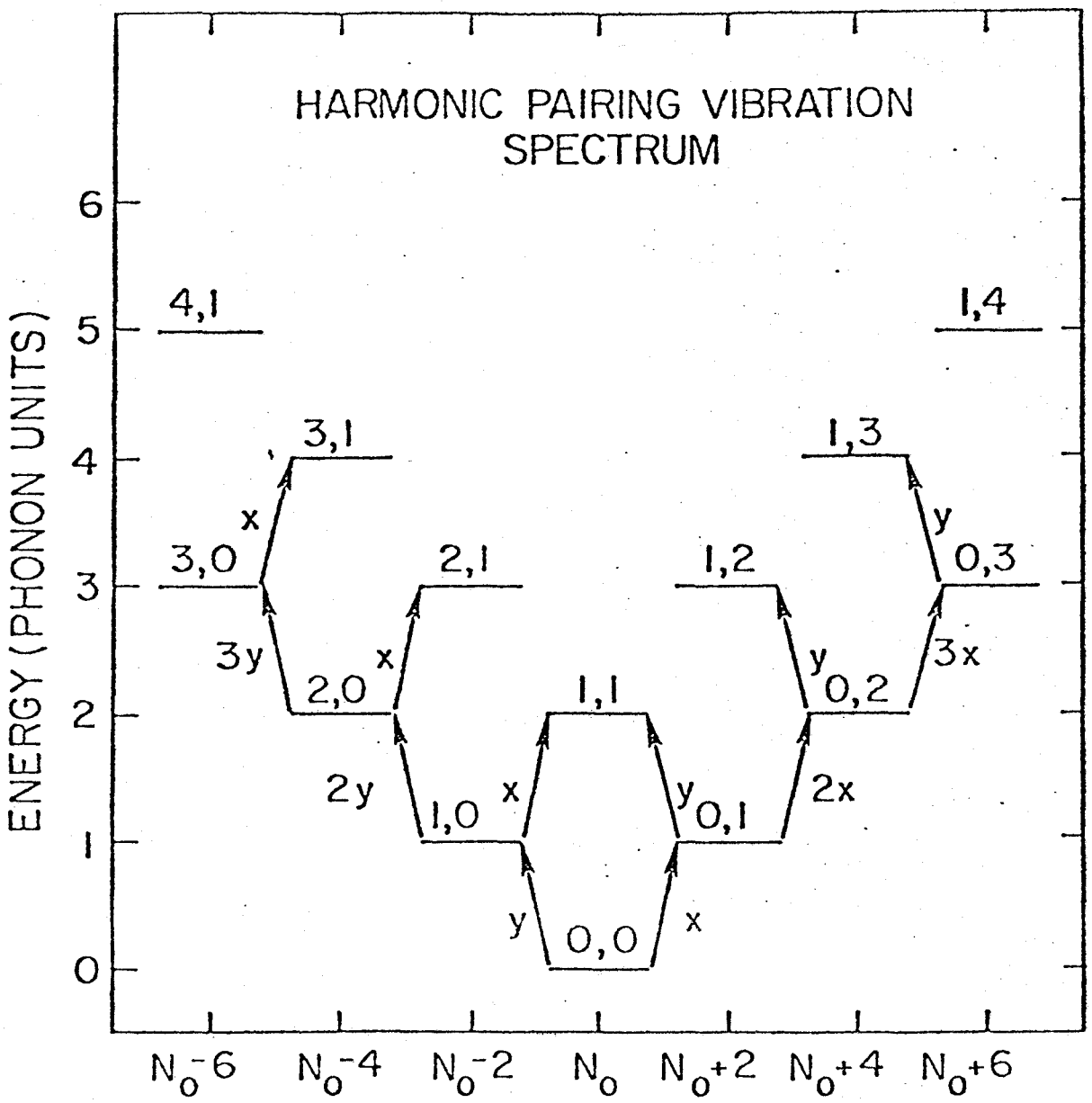
HARMONIC PAIRING VIBRATION SPECTRUM
ENERGY (PHONON UNITS)
0
1
2
3
4
5
6
4,1
1,4
3,1
1,3
3,0
2,1
1,2
0,3
2,0
1,1
0,2
1,0
0,1
0,0
x
y
3y
2y
2x
3x
N_o-6
N_o-4
N_o-2
N_o
N_o+2
N_o+4
N_o+6

poor. As well the model has no built in operator to handle inelastic scattering processes.

It seems that to fully explain the phenomenon of strongly populated excited states in these even-even nuclei a more detailed model calculation is required.

At present a calculation is being done on the ^{178}Yb and ^{180}Hf nuclei, by R. Griffin using a computer program he developed for the Volkov model (Griffin 1974).

APPENDIX A

TARGET PREPARATION

A.1 Yb Target

The mixture of Yb_2O_3 and thorium powder was compressed to form a pellet, placed in a tantalum crucible and heated to 1200°C in a vacuum of approximately 10^{-6} Torr. The thorium reduced the ytterbium oxide causing the subsequent production of ytterbium metal plus thorium oxide.

$$2\ Yb_2O_3 + 3\ Th \rightarrow 4\ Yb\uparrow + 3\ ThO_2$$

The carbon backing onto which the metal was evaporated was attached to a glass slide using a water soluble adhesive. Thus one was able to float the target off the plate and mount it onto an aluminum target frame.

The target used in the experiment was found to be 185 $\mu g/cm^2$ thick. This value was determined using the results of elastic scattering of tritons.

A.2 Sm Target

The ^{151}Sm target used in the experiment was manufactured in 1972 by R. D. Gadsby. The sample was produced in an Oak Ridge Isotope Separator in 1967. Because ^{151}Sm is radioactive, decaying by β^- emmission with a half-life of approximately 90 years, the purity of the target decreased over the years from 94.59% to 86.5% ^{151}Sm. Consequently there was a build up of the contaminant ^{151}Eu daughter in the target.

The preparation of the target was similar to that of the Yb target,

$$Sm_2O_3 + 2La \rightarrow La_2O_3 + 2Sm\uparrow \qquad \text{at } 1200°C.$$

There was virtually no lanthanum contamination as the vapour pressure of the lanthanum is appreciably less than that of samarium.

Prior to a final production of the ^{151}Sm target several test runs had been performed using a less expensive SmO_2 sample enriched in ^{152}Sm. However, even after cleaning and purging the crucible at 1500°C for 20 minutes some ^{152}Sm contamination did occur in the ^{151}Sm targets. Using a (d,d') reaction on ^{151}Sm the concentration of ^{152}Sm was found to be approximately 3 times that specified by the supplier (Gadsby 1972).

In the event of target breakage and subsequent contamination of the Enge target chamber a specialized container was developed to hold the target (Nelson 1971). As an added precaution the chamber was lined with aluminum foil.

Using elastic scattering of tritons the target thickness was determined to be 53 $\mu g/cm^2$, in good agreement with similar measurements made during earlier experiments with the same target.

A.3 Hf Target

The reduction of HfO_2 with Mg at 1000°C is complicated by the high vapour pressure of Mg. To prevent the Mg from evaporating out of the crucible a system was used whereby the Mg and its vapour were contained at a sufficiently high pressure so as to allow the process of reduction to take place in a reasonable length of time.

$$HfO_2 + 2\ Mg \rightarrow Hf + 2\ MgO$$

A pellet of Mg intimately mixed with HfO_2 was placed in a tantalum crucible and evacuated to a pressure of approximately 10^{-5} torr. The tantalum plug on the crucible was shaped so as to allow for a passage of air out of the crucible. The container was sealed by melting a band of nickel encircling the plug, using an electron gun.

The sealed unit was then placed in a quartz tube and heated in a tube furnace at 1000°C for 20 minutes. The contents of the crucible which include

Hf, Mg, MgO and a small residue of HfO_2, were removed from the container, and using a dilute solution of HCl the unwanted Mg and MgO were dissolved.

The resulting solution was decanted leaving a black powder of Hf with a yield of approximately 70%. A boat-type evaporation was used to prepare the target. Using elastic scattering results the target was found to be 153 $\mu g/cm^2$ thick.

REFERENCES

1. Bennett, M. J., Sheline, R. K., and Shida, Y., 1971. Nucl. Phys. A171, 113.
2. Bès, D. R., and Broglia, R. A., 1966. Nucl. Phys. 80, 289.
3. Bjerregaard, J. H., Hansen, O., Nathan, O., and Hinds, S., 1966. Nucl. Phys. 86, 145.
3. Broglia, R. A., and Riedel, C., 1967. Nucl. Phys. A92, 145.
4. Burke, D. G., Flynn, E. R., Sherman, J. D., and Sunier, J. W., 1976. Nucl. Phys. A258, 118.
5. Cairns, J. E., 1979. Private communication.
6. Flynn, E. R., Armstrong, D. D., Beery, J. A., and Blair, A. G., 1969. Phys. Rev. 182, 1113.
7. Gadsby, R. D., 1972. "A Study of the Reactions $^{149,151}Sm(p,t)^{147,149}Sm$". (McMaster University) M.Sc. Dissertation.
8. Glendenning, N. K., 1965. Phys. Rev. 137, 113.
9. Griffin, E. W., 1974. "A Self-Consistent 'Realistic' Pairing Theory with Applications to Two-Nucleon Transfer Reactions". (McMaster University) Ph.D. Dissertation.
10. Hammaren, E., 1978. Private communication. (Unpublished calculations).
11. Hintz, N. M., 1964. Nuclear Spectroscopy with Direct Reactions, II Proceedings, p. 425, Ed. Throw, F. E., Argonne National Laboratory, Chicago.
12. Katajanheimo, R., and Hammaren, E., 1978. Report Series in Physics HU-P-158, University of Helsinki, Finland.
13. Kenefick, R. A., and Sheline, R. K., 1965. Phys. Rev. 139, B1479.
14. Kuntz, P. D., 1974. University of Colorado, Computer Program DWUCK4, unpublished.

15. McLatchie, W., Reynolds, C. M., and Hintz, N. M., 1966. Phys. Rev. 151, 1000.

16. Mortensen, M. H., 1978. "The Collective Structure of the Tungsten Nuclei", (Yale University) Ph.D. Dissertation.

17. Nathan, O., 1968. Nuclear Structure Dubna Symposium, p. 191. International Atomic Energy Agency, Vienna.

18. Nelson, D. E., 1972. "The Nuclear Structure of ^{151}Sm". (McMaster University) Ph.D. Dissertation.

19. Nelson, D. E., Burke, D. G., Waddington, J. C., and Cook, W. B. 1973. Can. J. Phys. 51, 2000.

20. Nilsson, S. G., 1955. Mat. Fys. Medd. Dan. Vid. Selsk. 29, No. 16.

21. O'Neil, R. A., 1970. McMaster University, Computer Program SPECTR, unpublished.

22. Preston, M. A., and Bhaduri, R. K., 1975. Structure of the Nucleus, Addisson-Wesley Pub. Co. Inc., Reading, Mass.

23. Rekstad, J., Guttormsen, M., Engeland, T., Løvhøiden, G., Straume, O., Lien, J., and Ellegaard, C. E., 1978. "The ^{153}Sm Nucleus, an Experimental and Theoretical Study", to be published.

Guttormsen, M., Osnes E., Rekstad, J., Løvhøiden, G., and Straume, O., 1977. Nucl. Phys. A298, 122.

24. Rekstad, J., Private Communication to D. Burke (1978).

25. Robertson, R. G. H., Choh, S. H., Summers-Gill, R. G., and Stager, C. V., 1971. Can. J. Phys. 49, 766.

26. Spencer, J. E., and Enge, H. A., 1967. Nucl. Instr. and Meth. 49, 181.

27. Wapstra, A. H., and Bos, K., 1977. Nuclear Data Tables, Vol. 19, #3.

28. Westgaard, L., and Bjørnholm, S., 1966. Nucl. Instr. and Meth. 42, 77.